Comparative Properties of Transition Metal Catalysts Inferred from Activation Energies of Elementary Steps of Catalytic Reactions

Andrew V. Zeigarnik,[†,‡,§] Raúl E. Valdés-Pérez,[*,‡] and Jérôme Pesenti[‡]

Laboratory of Chemical Kinetics and Catalysis, Lomonosov Academy of Fine Chemical Technology, Moscow, 117571, Russia, and Department of Computer Science, Carnegie Mellon University, Pittsburgh, Pennsylvania 15213

Received: July 21, 1999; In Final Form: November 11, 1999

Experimental and calculated values of the activation energies of elementary steps provide insight into the mechanisms of many important catalytic reactions. The collections of these values also present an opportunity to apply *knowledge discovery* techniques in order to find more general qualitative patterns that are implicit in the data. Here, we apply classical hierarchical clustering and recently developed classification profiling methods to 168 steps and activation energies relevant to carbon dioxide re-forming of methane, compiled for eight different transition metal catalysts. The core fragments of the 168 transition states are defined and used as features. These methods and features address the basic questions of what the similarities and differences among catalysts are and why they are similar or different. The consistency of the results with experimental observations suggests that the methods are reliably predictive.

Introduction

A fundamental goal of theoretical catalysis is to discover patterns and trends in catalyst behavior and to predict catalyst activity. A key question is *why do certain catalysts behave similarly, while others are very different?* Knowledge of trends across the periodic table of the elements does not always help to answer this question. However, the energetics of elementary reactions may help fill the gap. Recent advances in the methods of quantum chemistry and quantum mechanics can provide fairly accurate predictions of activation and bond energies and reaction enthalpies. However, these raw calculated (or experimental) data do not directly help us understand chemical processes, and it remains unclear what would be a reliable general method for inferring the trends of catalyst behavior from these data.

This article shows that standard and recently designed knowledge discovery techniques[1] are helpful for making the fundamental properties of transition metal catalysts in heterogeneous catalysis more explicit and understandable. We illustrate the approach by using previously calculated activation energies of 168 elementary reactions for eight different single-crystal transition metal catalysts.[2] The set of elementary steps cover the essential chemistry of CO_2 and steam re-forming of methane, the water gas shift reaction, methanol synthesis, and some other reactions of C_1-C_2 chemistry. The methods used in this paper to uncover patterns in the calculated data are two standard clustering algorithms that enable finding of families of similar metal catalysts, and a new method that enables finding of the most contrasting features of elements from the different families. To the best of our knowledge, this is one of the very few applications of knowledge discovery or data mining to catalysis.

* To whom correspondence should be addressed. E-mail: valdes@cs.cmu.edu.
† Lomonosov Academy of Fine Chemical Technology.
‡ Carnegie Mellon University.
§ E-mail: azeigarn@dol.ru.

Methods

Two computational methods were used, one familiar (clustering) and one new (profiling). We used classical hierarchical clustering,[3] whose starting point is a list of objects and the distances between each pair of objects. These clustering methods are bottom-up or agglomerative. They begin by defining each object as a cluster by itself and then proceed by repeatedly merging the two nearest clusters to form a new cluster. The result is a hierarchy of clusters that is a binary tree (i.e., each node of the tree splits into two descendants). The leaves of this tree contain the initial objects, the root contains all objects, and any intermediate node corresponds to the merging of the two nodes below it.

The several variants of hierarchical clustering differ by the measure of distance between two *clusters* of objects. The three most common measures are the distances between (1) the two farthest members of each cluster (complete-link), (2) the two nearest members of each cluster (single-link), and (3) the mean of the distances between every pair of objects each taken from a different cluster (average-link). Each variant has advantages and disadvantages. Below we use single-link and complete-link clustering; average-link gave results similar to complete-link.

The second method used here was recently developed.[4] Given a set of classes, each represented by some number of members, where each member is described by numeric or symbolic features, the concise all-pairs profiling (CAPP) method profiles each class by listing a minimal set of features that contrast that class from the other classes. A novel aspect of this method is that it explicitly compares all pairs of classes, constructs a logical formula that expresses the alternative possible contrasts, and then manipulates this formula to extract a minimal set of features needed to profile each of the classes. By default, the method minimizes the overall use of features for all class profiles jointly; an alternative is to minimize the profile for each class separately, which is the option used in this article. When features take on numeric values, two classes are contrasted by collecting the

10.1021/jp992520q CCC: $19.00
Published on Web 01/15/2000

feature values for each class into sorted lists and then calculating the extent (normalized to between 0 and 1) of overlap between the two lists. An advantage of this contrast measure (overlap) is that it is nonparametric (makes no distributional assumptions), and it can be used analogously on symbolic (unordered) features.

In what follows, we use the term "feature" somewhat ambiguously. Propositions of the form "step has property X" (e.g., step forms methanol) will be called features, even though they more properly should be called selectors, since they serve to select a subset of steps that have the property X. At the same time, the "activation energy of a step that has property X" will also be called a feature. The context will make clear whether step selection or numerical attribution is involved.

Initial Data and Reliability Issues

Our starting data consist of 168 elementary steps (Table 1) and their activation energies for eight single-crystal catalysts taken from ref 2. These activation energies were calculated using the unity bond index quadratic exponential potential (UBI-QEP) method,[5] formerly known as the bond-order conservation Morse potential (BOC-MP) method.[6,7] The accuracy of these calculations was claimed to be 1−3 kcal/mol. The single-crystal catalysts are Cu(111), Ni(111), Pd(111), Pt(111), Rh(111), Ru(001), Ir(111), and Fe(110).[2] For each of the steps we defined features that can be used to contrast these metal catalysts (see next section).

General Reliability Problems. The problem of reliability of the initial data set is important. The more reliable the input, the more plausible the hypotheses that are the outcome of mining this data set. We did not recalculate and check all the entries of Table 1. When comparing the UBI-QEP data with experimental values or other calculations, we also faced several problems. (1) Experimental data are not always available for single-crystal faces. This is the most common problem. (2) The available experimental data may be unreliable. (3) Some of the experimental activation energies are apparent. That is, they refer to nonsingle step processes, such as physisorption/sticking plus dissociation or diffusion plus recombination, etc. This difference is most pronounced when comparing the values for adsorption/desorption steps. (4) The calculated activation energies are for zero surface coverage, and experimental data are often for nonzero coverages. The difference is often significant.

The interpretation of experiments due to the factors listed above is difficult and results in a wide range of activation energies for the same reaction. For instance, for water formation on the surface from adsorbed hydroxyl and hydrogen on Pt(111), the range of reported activation energies is 2−20 kcal mol.[8]

The qualitative comparison of trends for any specific step can also be difficult because the rate of any specific reaction sometimes correlates poorly with the intrinsic activation energy because of the preexponential factor in the Arrhenius rate law. Even qualitative data for single crystals are scarce.

Direct comparisons of a set of single crystal faces to real catalysts are not fully correct for various reasons. An important factor is the effect of support. Another factor is surface structure sensitivity.[9] In real catalysts, the same catalyst may contain various single-crystal faces of the same metal. They do not necessarily show the same activity. Often the activity of different faces is different. A striking example is ammonia synthesis over different surfaces of iron: Fe(111) is over 6 times more active than Fe(100), and the activity of Fe(110) is miserable relative to the activity of Fe(111) and Fe(100).[10] So when applying the techniques described in this paper, one should not forget that the clustering results may be different if we consider other faces of the same metals.

Hei et al.[2] reported comparisons for several reactions, and we also compared calculated and experimental data. This information is presented below.

C_2H_5−H Dissociation. Hei et al.[2] compared the data on ethane dissociation on Ir(111)[11] and Pt(111).[12] The experimental values coincided with the UBI-QEP values within 3 kcal/mol error, but this reaction was not included in the list. Rather, Hei et al.[2] used these data in their own calculations.

CH_3−H Dissociation. The activation energies for methane dissociation listed in Table 1 are the values for the reaction occurring on the surface $CH_{4,s} \rightarrow CH_{3,s} + H_s$. To compare to the literature data, we should estimate apparent activation energies for $CH_{4,g} \rightarrow CH_{3,s} + H_s$. To a first approximation, this can be done by subtracting the values of the methane heat of adsorption without dissociation: $E_{CH4,g} = E_{CH4,s} - Q_{CH4}$.[6] Table 2 summarizes the data for methane dissociative adsorption from the gas phase and methane dissociation on the surface. The activation energy of dissociation and adsorption heats are taken from ref 2.

According to Zaera,[20] the activation barrier for the dissociation of alkanes on metal surfaces in most cases is lower than 20 kcal/mol. All UBI-QEP values for methane dissociation (the first line in Table 1) are between 8.2 kcal/mol for Fe(110) and 18.1 for Ir(111), with the exception of Cu(111) for which the value is 29.4 kcal/mol.

Beebe et al.[14a] measured the kinetics of methane dissociative adsorption on Ni(111) and found an activation energy of 12.6 ± 1.2 kcal/mol. The reaction order with respect to methane partial pressure was found to be fractional. Therefore, the process of methane dissociative adsorption is not a direct process. The authors reported excellent agreement of their measurements with molecular beam findings of Lee et al.[14b] The results obtained by Ceyer and co-workers using supersonic molecular beam techniques and HREELS also agree with the value of 12 kcal/mol.[14b,c,d] Dissociative chemisorption of methane on Ni(111) was also reviewed by Whitten and Yang.[21] Various theoretical studies report slightly overestimated values between 15 and 17 kcal/mol.[5,21] DFT methods strongly overestimate the activation energy especially if small clusters are chosen.

Schoofs et al.[15] carried out a molecular beam study of methane dissociative adsorption on Pt(111) and interpreted the data reported by others for Ni(111), Ir(110), and W(110). They showed that methane dissociative adsorption on the surface is direct. Activation barriers calculated from the experimental data fall in the range 23.6−28.9 kcal/mol and agree well with analogous UBI-QEP values calculated using the model of one-dimensional energy profile. According to Shustorovich,[6] that model typically gives overestimated values. If molecular beam data are treated considering one-dimensional barriers, the calculated activation barriers are usually too high. To correct the data, we should use the formula recommended by Shustorovich:[6]

$$E_{corr} = (^1/_2)(E_{exptl} - Q_{CH4})$$

Then the activation energies for Ni(111) and Pt(111) become 8.8 and 11.5 kcal/mol, respectively. These values derived from experiment agree well with UBI-QEP calculations (7.8 and 11.7 kcal/mol). Valden et al.[17] reported the results of a molecular beam surface scattering study, including two values for Pt(111). One is thermal barrier height (58 ± 1 kcal/mol), which is higher

TABLE 1: Elementary Steps Taken Entirely from Ref 2 and Their Activation Energies (in kcal/mol) for Cu(111), Ni(111), Pd(111), Pt(111), Rh(111), Ru(001), Ir(111), and Fe(110)[a]

no.	step	Cu	Ni	Pd	Pt	Rh	Ru	Ir	Fe
1	$CH_4 \rightarrow CH_3 + H$	29.4	13.8	15.9	17.7	14.7	10.6	18.1	8.2
2	$CH_3 \rightarrow CH_2 + H$	32.1	23.9	24.8	25.7	24.6	22.0	26.2	21.7
3	$CH_2 \rightarrow CH + H$	26.6	23.2	23.8	24.4	23.9	21.9	25.0	22.3
4	$CH \rightarrow C + H$	7.4	4.5	4.9	5.4	4.9	3.5	5.9	3.7
5	$CH_3 + CH_2 \rightarrow CH_4 + CH$	4.5	17.7	14.4	11.7	17.5	20.5	13.9	27.3
6	$CH_3 + CH \rightarrow CH_4 + C$	0.0	0.0	0.0	0.0	0.0	1.4	0.0	8.7
7	$CH + CH \rightarrow CH_2 + C$	0.0	7.7	5.0	2.5	7.3	10.0	5.0	14.8
8	$CH_4 + CH_2 \rightarrow CH_3 + CH_3$	1.3	0.0	0.0	0.0	0.0	0.0	0.0	0.0
9	$CH_2 + CH_2 \rightarrow CH_3 + CH$	6.8	17.5	15.0	12.9	17.3	19.6	15.0	24.4
10	$CH_2 + CH \rightarrow C + CH_3$	0.0	0.0	0.0	0.0	0.0	2.2	0.0	7.7
11	$CH_2 + CH_2 \rightarrow C_2H_4$	0.0	6.5	0.0	0.0	6.0	14.3	0.0	31.1
12	$CH_3 + CH_3 \rightarrow C_2H_6$	0.0	13	6.5	0.9	12.4	18.5	6.5	30.4
13	$C_2H_6 + CH_3 \rightarrow C_2H_5 + CH_4$	0.0	0.0	0.0	0.0	0.0	0.0	0.0	0.0
14	$C_2H_5 + CH_3 \rightarrow C_2H_4 + CH_4$	0.0	16.2	10.5	5.7	15.7	20.9	10.0	31.6
15	$CO_2 + CH_3 \rightarrow CH_3O + CO$	5.5	9.5	12.7	11.7	11.7	15.6	11.2	13.4
16	$CO_2 + CH_2 \rightarrow CH_2O + CO$	0.0	0.0	0.0	0.0	0.0	2.1	0.0	5.6
17	$CO_2 + CH \rightarrow CO + HCO$	0.0	0.0	0.0	0.0	0.0	0.0	0.0	0.0
18	$CO_2 + C \rightarrow CO + CO$	0.0	0.0	0.0	0.0	0.0	1.1	0.0	6.1
19	$CO_2 + O \rightarrow CO + O_2$	83.4	77.5	49.0	49.4	62.6	64.1	53.7	80.8
20	$CO_2 + H \rightarrow HCOO$	3.7	2.8	21.0	21.5	8.2	15.8	12.4	2.1
21	$CO_2 + H \rightarrow CO + OH$	6.4	4.8	9.3	9.7	5.1	9.5	5.6	1.9
22	$CO_2 + H \rightarrow HCO + O$	41.5	24.7	44.3	49.8	29.0	31.4	34.9	21.4
23	$CO_2 + OH \rightarrow HOO + CO$	61.2	43.2	39.3	41.8	41.1	44.1	39.3	41.3
24	$CO + H \rightarrow C + OH$	38.1	24.8	37.3	40.7	28.5	25.8	34.3	13.3
25	$CO_2 \rightarrow CO + O$	17.3	6.7	17.1	18.4	11.3	12.7	14.6	4.5
26	$CO \rightarrow C + O$	50.7	33.4	50.2	54.1	40.4	35.1	48.4	24.6
27	$CH_4 + O \rightarrow CH_3 + OH$	16.7	14.0	9.2	10.1	10.6	8.6	10.9	8.6
28	$CH_4 + O \rightarrow CH_3O + H$	20.4	20.2	14.3	14.2	18.3	15.4	17.9	20.4
29	$CH_3 + O \rightarrow CH_2 + OH$	22.9	25.1	18.0	17.9	21.1	20.1	19.5	23.4
30	$CH_3 + O \rightarrow CH_3O$	2.1	20.9	12.6	8.9	18.6	21.8	13.6	32.0
31	$CH_2 + O \rightarrow CH_2O$	0.0	24.2	6.0	0.4	17.8	21.7	8.8	39.8
32	$CH_2 + O \rightarrow CH + OH$	21.5	25.1	17.0	16.5	20.9	20.2	18.6	24.7
33	$CH_2 + O \rightarrow HCO + H$	4.5	20.9	0.0	0.0	17.6	11.1	7.7	28.8
34	$CH + O \rightarrow C + OH$	3.4	7.3	0.0	0.0	2.6	1.8	0.0	7.4
35	$CH + O \rightarrow CO + H$	0.0	11.4	0.0	0.0	1.0	3.7	0.0	24.2
36	$CH_4 + H \rightarrow CH_3 + H_2$	31.9	15.6	20.0	23.7	14.5	14.4	16.8	4.0
37	$CH_3 + H \rightarrow CH_2 + H_2$	34.7	27.2	29.2	30.9	25.8	28.1	26.0	20.8
38	$CH_2 + H \rightarrow CH + H_2$	24.4	20.8	21.8	22.8	19.5	22.6	18.6	17.4
39	$CH + H \rightarrow C + H_2$	5.3	9.5	8.9	8.3	8.2	12	6.5	10.1
40	$CH_4 + OH \rightarrow CH_3 + H_2O$	25.6	9.6	4.3	6.1	7.0	4.0	6.8	5.2
41	$CH_3 + OH \rightarrow CH_3O + H$	13.1	21.0	17.5	15.6	21.8	21.7	19.8	29.7
42	$CH_3 + OH \rightarrow CH_2 + H_2O$	28.3	18.5	9.8	11.7	14.9	11.3	12.9	15.9
43	$CH_2 + OH \rightarrow CH + H_2O$	18.1	13.3	5.9	6.2	10.2	8.8	8.0	13.8
44	$H_2COH \rightarrow CH_2 + OH$	33.7	27.0	19.7	22.1	18.7	15.4	20.4	11.8
45	$H_2COH \rightarrow CH + H_2O$	51.8	14.2	8.8	16.3	9.9	4.7	11.8	2.5
46	$CH_3O \rightarrow CH_2O + H$	8.7	9.5	0.4	0.3	6.0	2.4	4.4	10.1
47	$CH_3O + C \rightarrow CH_3 + CO$	4.0	20.4	0.0	0.0	9.6	12.7	0.2	25.9
48	$CH_3O + CH \rightarrow CH_2 + CH_2O$	0.0	20	6.5	4.4	14.2	14.6	9.1	24.9
49	$CH_3O + CH \rightarrow CH_3 + HCO$	1.1	10.7	0.0	0.0	3.0	2.1	0.0	12.1
50	$CH_3O + CH_2 \rightarrow CH_3 + CH_2O$	0.0	14.2	1.2	0.0	9.0	10.0	3.5	20.9
51	$CH_3O + CH_3 \rightarrow CH_2 + CH_3OH$	27.1	7.8	7.6	8.1	11.6	9.7	9.6	19.8
52	$CH_3O + CH_3 \rightarrow CH_4 + CH_2O$	0.0	15.6	2.8	0.0	10.9	13.3	4.3	26.1
53	$CH_3O + O \rightarrow CH_3 + O_2$	82.3	77.6	42.5	44.4	59.3	51.5	51.1	77.3
54	$CH_3O + OH \rightarrow CH_3OH + O$	10.0	11.5	6.3	6.1	9.7	9.2	7.6	13.8
55	$CH_2O \rightarrow HCO + H$	19.9	10.6	9.1	10.8	9.8	5.3	11.5	5.2
56	$CH_2O + CH_3O \rightarrow CH_3OH + HCO$	12.2	6.8	0.0	0.0	0.5	0.0	0.0	0.8
57	$CH_2O + O \rightarrow OH + HCO$	25.2	12.4	4.8	6.4	7.7	4.6	7.0	6.0
58	$C + CH_2O \rightarrow CH_2 + CO$	5.8	9.5	0.0	0.0	3.6	5.9	0.0	9.5
59	$CH_3 + CH_2O \rightarrow CH_4 + HCO$	0.2	3.4	0.0	0.0	0.6	0.2	0.0	4.2
60	$CH_3OH \rightarrow CH_3O + H$	17.8	13.2	17.8	18.5	16.1	14.6	18.6	12.4
61	$CH_3OH + H \rightarrow CH_3 + H_2O$	8.8	2.6	2.1	3.6	0.6	1.0	0.6	0.0
62	$HCOO \rightarrow CO + OH$	5.3	5.3	0.0	0.0	1.1	1.7	0.0	3.2
63	$HCOO \rightarrow HCO + O$	39.2	25.2	26.4	28.3	24.9	23.6	26.3	21.2
64	$HCOO + CH \rightarrow CH_2 + CO_2$	4.1	19.5	1.1	0.0	11.3	11.4	4.6	25.2
65	$HCOO + CH \rightarrow HCO + HCO$	0.0	2.3	0.0	0.0	1.3	6.5	0.0	15.8
66	$HCOO + CH_3 \rightarrow HCO + CH_3O$	22.8	25.9	20.9	20.1	23.6	24.0	21.8	28.4
67	$HCOO + CH_3 \rightarrow CH_4 + CO_2$	0.0	14.4	0.0	0.0	7.5	9.6	0.0	25.6
68	$HCOO + H \rightarrow H_2 + CO_2$	14.0	24.6	9.2	7.7	17.0	19.0	10.0	27.0
69	$HCOO + O \rightarrow OH + CO_2$	0.0	2.6	0.0	0.0	0.0	0.0	0.0	2.8
70	$HCO \rightarrow CO + H$	0.0	0.0	0.0	0.0	0.0	0.0	0.0	2.6
71	$HCO \rightarrow CH + O$	0.0	22.9	1.7	0.0	14.2	16.0	5.6	33.2
72	$HCO + O \rightarrow CO + OH$	0.0	0.0	0.0	0.0	0.0	0.0	0.0	3.0
73	$HCO + CH_3O \rightarrow CH_3OH + CO$	0.0	5.3	0.0	0.0	0.0	1.9	0.0	11.5

TABLE 1: Continued[a]

no.	step	Cu	Ni	Pd	Pt	Rh	Ru	Ir	Fe
74	$HCO + CH_3 \rightarrow CH_4 + CO$	0.0	0.5	0.0	0.0	0.0	0.0	0.0	14.6
75	$HCO + CH \rightarrow CH_2 + CO$	0.0	3.2	0.0	0.0	0.5	6.6	0.0	13.2
76	$HCO + H \rightarrow CO + H_2$	0.0	10.0	2.5	0.0	6.5	14.0	0.5	15.7
77	$HCO + CH_2 \rightarrow CH_3 + CO$	0.0	0.0	0.0	0.0	0.0	1.8	0.0	9.2
78	$HCO + CH_3O \rightarrow CH_2O + CH_2O$	1.6	19.6	10.3	6.9	16.9	19.3	11.6	30.0
79	$OH + OH \rightarrow O + H_2O$	11.5	11.5	8.0	8.0	11.2	10.8	9.3	15.4
80	$OH + H \rightarrow H_2O$	13.8	20.7	12.2	11.2	16.8	19.9	11.8	24.1
81	$OH + H_2 \rightarrow H + H_2O$	2.3	2.2	0.0	0.0	0.0	0.0	0.0	4.4
82	$H + O \rightarrow OH$	10.7	19.4	11.6	10.3	14.1	17.8	10.2	19.1
83	$OH + H \rightarrow O + H_2$	17.3	17.2	26.4	26.6	21.6	26.9	21.6	20.2
84	$H + H \rightarrow H_2$	10.6	23.4	22.2	21.1	21.1	27.9	17.6	24.5
85	$CH_3 + H \rightarrow CH_4$	0.0	13.4	9.3	5.6	11.8	18.6	6.4	23.4
86	$CH_2 + H \rightarrow CH_3$	0.0	11.9	9.0	6.4	10.4	16.3	6.4	17.9
87	$CH + H \rightarrow CH_2$	4.8	17.6	15.4	13.2	16.0	21.7	12.6	21.9
88	$C + H \rightarrow CH$	30.8	41.5	39.7	38.0	39.9	45.4	36.7	44.7
89	$CH_4 + CH \rightarrow CH_3 + CH_2$	12.1	12.5	12.6	12.6	12.5	12.3	13.1	11.7
90	$CH_4 + C \rightarrow CH_3 + CH$	53.0	37.0	41.0	45.0	38.0	35.3	42.0	34.5
91	$CH_2 + C \rightarrow 2CH$	45.2	50.3	48.2	46.3	50.2	52.1	48.2	56.2
92	$CH_3 + CH_3 \rightarrow CH_4 + CH_2$	4.0	11.6	9.2	7.2	11.3	13.7	8.2	19.0
93	$CH_3 + CH \rightarrow CH_2 + CH_2$	17.0	23.9	22.4	21.0	23.6	25.1	22.4	27.8
94	$C + CH_3 \rightarrow CH_2 + CH$	55.0	49.0	51.0	52.0	49.0	49.8	51.0	52.5
95	$C_2H_4 \rightarrow 2CH_2$	84.6	33.5	36.1	48.5	33.8	29.1	36.1	19.8
96	$C_2H_6 \rightarrow 2CH_3$	40.6	10.8	14.7	18.1	11.2	7.5	14.7	0.0
97	$C_2H_5 + CH_4 \rightarrow C_2H_6 + CH_3$	9.7	9.2	9.1	9.0	9.2	9.2	9.1	9.5
98	$C_2H_4 + CH_4 \rightarrow C_2H_5 + CH_3$	28.7	7.9	10.9	13.5	8.2	5.4	11.4	0.0
99	$CH_3O + CO \rightarrow CO_2 + CH_3$	4.4	9.6	6.2	6.4	8.4	3.1	8.6	10.0
100	$CH_2O + CO \rightarrow CO_2 + CH_2$	25.9	7.9	18.3	23.1	11.4	2.8	19.2	1.1
101	$CO + HCO \rightarrow CO_2 + CH$	27.9	20.2	34.5	36.8	27.6	20.2	33.9	17.9
102	$CO + CO \rightarrow CO_2 + C$	28.5	6.4	34.1	40.3	18.6	3.9	33.5	0.9
103	$CO + O_2 \rightarrow CO_2 + O$	0.0	0.0	0.0	0.0	0.0	0.0	0.0	0.0
104	$HCOO \rightarrow CO_2 + H$	1.3	3.5	0.0	0.0	0.0	0.0	0.0	4.4
105	$CO + OH \rightarrow CO_2 + H$	3.9	15.3	12.5	11.1	16.9	11.0	16.7	21.3
106	$HCO + O \rightarrow CO_2 + H$	0.0	10.2	0.0	0.0	4.2	3.9	0.0	20.6
107*	$HOO + CO \rightarrow CO_2 + OH$	0.0	0.0	0.0	0.0	0.0	0.0	0.0	0.0
108	$C + OH \rightarrow CO + H$	6.9	28.8	6.3	1.7	21.5	24.3	11.7	45.6
109	$CO + O \rightarrow CO_2$	0.0	15.2	7.3	4.8	13.1	9.7	10.3	20.6
110	$C + O \rightarrow CO$	4.7	35.4	6.2	0.1	23.4	29.1	10.4	49.6
111	$CH_3 + OH \rightarrow CH_4 + O$	2.1	15.6	15.6	13.0	17.7	21.1	14.7	27.1
112	$CH_3O + H \rightarrow CH_4 + O$	7.4	11.7	11.0	10.5	10.5	14.1	8.2	12.3
113	$CH_2 + OH \rightarrow CH_3 + O$	5.6	15.1	15.2	13.6	16.9	18.9	15.1	22.9
114	$CH_3O \rightarrow CH_3 + O$	18.4	12.8	15.9	17.3	13.7	12.4	15.5	8.7
115	$CH_2O \rightarrow CH_2 + O$	43.4	23.9	34.2	37.2	27.6	25.5	32.6	15.6
116	$CH + OH \rightarrow CH_2 + O$	14.4	21.5	21.4	20.3	23.1	24.4	21.4	27.9
117	$HCO + H \rightarrow CH_2 + O$	28.0	27.2	36.0	39.5	27.8	35.2	33.7	26.5
118	$C + OH \rightarrow CH + O$	41.6	46.3	48.0	47.6	47.5	48.3	46.4	51.4
119	$CO + H \rightarrow CH + O$	69.4	46.4	78.8	86.6	53.0	51.6	68.8	40.2
120	$CH_3 + H_2 \rightarrow CH_4 + H$	0.0	0.0	0.0	0.0	0.0	0.0	0.0	2.3
121	$CH_2 + H_2 \rightarrow CH_3 + H$	0.0	0.0	0.0	0.0	0.0	0.0	0.0	0.0
122	$CH + H_2 \rightarrow CH_2 + H$	0.0	0.0	0.0	0.0	0.0	0.0	0.0	0.0
123	$C + H_2 \rightarrow CH + H$	26.1	31.3	30.3	29.3	31.6	31.5	31.1	34.1
124	$CH_3 + H_2O \rightarrow CH_4 + OH$	0.0	2.7	3.7	1.6	3.4	6.4	2.1	8.3
125	$CH_3O + H \rightarrow CH_3 + OH$	14.7	10.9	7.9	9.0	6.9	7.8	6.3	3.1
126	$CH_2 + H_2O \rightarrow CH_3 + OH$	0.0	0.0	0.0	0.0	0.0	0.0	0.0	0.0
127	$CH + H_2O \rightarrow CH_2 + OH$	0.0	1.2	3.3	2.6	1.7	2.9	2.3	1.6
128	$CH_2 + OH \rightarrow H_2COH$	0.0	8.0	13.5	9.4	19.4	23.6	14.1	34.6
129	$CH + H_2O \rightarrow H_2COH$	0.0	0.2	0.3	0.0	2.0	7.0	0.0	12.8
130	$CH_2O + H \rightarrow CH_3O$	3.7	5.3	9.5	9.3	6.5	9.9	6.4	5.3
131	$CH_3 + CO \rightarrow CH_3O + C$	33.7	26.5	40.6	45.6	31.5	28.1	36.3	24.2
132	$CH_2 + CH_2O \rightarrow CH_3O + CH$	17.0	21.4	24.0	24.6	22.6	22.3	23.6	20.6
133	$CH_3 + HCO \rightarrow CH_3O + CH$	30.1	30.8	41.0	42.1	33.9	34.9	36.5	33.4
134	$CH_3 + CH_2O \rightarrow CH_3O + CH_2$	24.4	22.0	26.0	21.2	23.7	23.2	25.4	19.9
135	$CH_2 + CH_3OH \rightarrow CH_3O + CH_3$	0.0	0.0	1.7	2.1	1.4	1.6	3.2	0.0
136	$CH_4 + CH_2O \rightarrow CH_3O + CH_3$	24.2	11.8	18.5	7.0	14.3	12.8	18.0	6.1
137	$CH_3 + O_2 \rightarrow CH_3O + O$	0.0	0.0	0.0	0.0	0.0	0.0	0.0	0.0
138	$CH_3OH + O \rightarrow CH_3O + OH$	3.1	4.1	3.6	3.4	3.2	3.3	3.4	2.5
139	$HCO + H \rightarrow CH_2O$	0.0	17.2	16.8	13.3	17.5	24.7	13.7	27.1
140	$CH_3OH + HCO \rightarrow CH_2O + CH_3O$	0.2	8.0	18.1	14.9	11.7	17.9	13.5	8.4
141	$OH + HCO \rightarrow CH_2O + O$	0.0	4.1	5.6	3.6	6.0	8.5	4.6	11.2
142	$CH_2 + CO \rightarrow C + CH_2O$	8.3	7.8	15.8	17.2	10.8	8.1	14.3	8.8
143	$CH_4 + HCO \rightarrow CH_3 + CH_2O$	9.6	10.4	14.4	14.6	11.2	11.5	13.9	11.0
144	$CH_3O + H \rightarrow CH_3OH$	9.9	18.6	7.5	6.2	12.6	15.5	7.4	20.4
145	$CH_3 + H_2O \rightarrow CH_3OH + H$	3.0	11.5	7.4	5.5	11.3	10.7	9.7	22.5
146	$CO + OH \rightarrow HCOO$	4.9	14.7	24.1	22.8	20.9	18.8	23.3	20.0
147	$HCO + O \rightarrow HCOO$	0.0	9.6	3.1	0.0	8.7	11.7	3.8	20.8

TABLE 1: Continued[a]

no.	step	Cu	Ni	Pd	Pt	Rh	Ru	Ir	Fe
148	$CH_2 + CO_2 \rightarrow HCOO + CH$	28.3	24.3	30.5	32.7	27.4	27.4	29.4	23.3
149	$HCO + HCO \rightarrow HCOO + CH$	49.5	28.1	31.3	36.1	28.7	27.5	31.3	26.6
150	$HCO + CH_3O \rightarrow HCOO + CH_3$	0.0	2.2	1.0	0.2	2.4	2.8	1.2	4.6
151	$CH_4 + CO_2 \rightarrow HCOO + CH_3$	32.0	14.0	28.0	34.0	18.6	17.4	14.0	8.1
152	$H_2 + CO_2 \rightarrow HCOO + H$	14.3	8.7	16.8	17.6	13.2	12.0	16.0	7.4
153	$OH + CO_2 \rightarrow HCOO + O$	16.9	3.5	33.9	36.4	18.0	20.1	27.6	3.5
154	$CO + H \rightarrow HCO$	24.0	23.0	34.4	36.1	26.0	24.5	30.4	20.5
155	$CH + O \rightarrow HCO$	45.4	34.9	46.1	50.5	40.0	39.4	44.0	31.3
156	$CO + OH \rightarrow HCO + O$	38.8	25.1	47.4	51.1	36.6	29.0	45.8	20.2
157	$CH_3OH + CO \rightarrow HCO + CH_3O$	32.0	22.9	45.0	48.0	30.0	24.9	42.0	21.5
158	$CH_4 + CO \rightarrow HCO + CH_3$	53.4	23.9	41.0	48.2	28.9	16.5	42.0	17.3
159	$CH_2 + CO \rightarrow HCO + CH$	45.9	31.8	43.0	47.3	34.4	31.3	43.0	31.5
160	$CO + H_2 \rightarrow HCO + H$	25.5	17.8	23.5	24.5	20.9	16.1	24.7	16.6
161	$CH_3 + CO \rightarrow HCO + CH_2$	56.1	35.0	50.2	55.4	40.2	32.0	50.2	30.9
162	$CH_2O + CH_2O \rightarrow HCO + CH_3O$	16.5	8.6	11.6	13.4	9.1	7.5	11.4	3.1
163	$O + H_2O \rightarrow 2OH$	0.5	3.0	1.0	0.6	0.5	0.7	0.8	0.0
164	$H_2O \rightarrow OH + H$	17.6	14.2	18.2	18.8	16.1	14.3	18.7	12.0
165	$H + H_2O \rightarrow OH + H_2$	8.6	10.9	19.4	19.2	10.9	16.8	13.1	9.2
166	$OH \rightarrow H + O$	25.5	21.4	24.6	25.3	24.1	22.3	25.6	22.4
167	$O + H_2 \rightarrow OH + H$	0.0	0.0	0.0	0.0	0.0	0.0	0.0	0.0
168	$H_2 \rightarrow H + H$	15.4	8.2	8.8	9.5	9.5	5.6	11.4	7.0

[a] Reactions 23 and 107 are irrelevant to methane re-forming with CO_2 because the OOH species to the best of our knowledge was not formed during the reaction. Reactions 45, 62, 129, and 146 have excessively complex transition states.

TABLE 2: Activation Energies (in kcal/mol) of Methane Dissociative Adsorption and Dissociation on the Surface

reaction	Cu(111)	Ni(111)	Pd(111)	Pt(111)	Rh(111)	Ru(001)	Ir(111)	Fe(110)
				Experiment				
$CH_{4,g} \rightarrow CH_{3,s} + H_s$	48[a]	12.6 ± 1.2[b] 8.8[c]	8[d]	6.2 ± 2.4[e] 11.5[c]		8.8[h]	6.5 ± 0.9[f] 17.4−18.1[g]	
				UBI-QEP				
$CH_{4,g} \rightarrow CH_{3,s} + H_s$	23.4	7.8	9.9	11.7	8.7	4.6	11.1	2.2
$CH_{4,s} \rightarrow CH_{3,s} + H_s$	29.4	13.8	15.9	17.7	14.7	10.6	18.1	8.2

[a] Reference 13. [b] Reference 14. [c] Reference 15. [d] Reference 16. [e] Reference 17. [f] Reference 18. [g] Reference 19. [h] Larsen, J. H.; Holmlad, P. M.; Chorkendorff, I. *J. Chem. Phys.* **1999**, *110*, 2637.

TABLE 3: Activation Energies (in kcal/mol) of Hydrogen Dissociative Adsorption and Dissociation on the Surface

reaction	Cu(111)	Ni(111)	Pd(111)	Pt(111)	Rh(111)	Ru(001)	Ir(111)	Fe(110)
				Experiment				
$H_{2,g} \rightarrow 2H_s$	5[a]	1−2[b]		1[c]		0[c]		0[c,d]
				UBI-QEP				
$H_{2,g} \rightarrow 2H_s$	7.2	1.3	2.2	3	3	0	5.6	0.4
$H_{2,s} \rightarrow 2H_s$	15.4	8.2	8.8	9.5	9.5	5.6	11.4	7.0

[a] References 24 and 25. [b] References 21 and 26. [c] Reference 5. [d] Reference 27. The initial sticking coefficient and the rate of adsorption were found to be independent of temperature.

than the apparent activation barrier for methane dissociative adsorption. The other value (6.3 ± 2.4 kcal/mol) is the apparent activation energy calculated using the statistical approach proposed by Ukraintev and Harrison.[22] The latter value was claimed to be unreliable.

Seets et al.[18] reported an activation energy for methane dissociative adsorption on Ir(111) of 6.5 kcal/mol, which was obtained by molecular beam and bulb gas techniques. Jachimowski et al.[19] measured the activation energies for $^{13}CH_4$ and CD_4 dissociative adsorption and obtained 17.4 and 18.1 kcal/mol, respectively. That is, in these cases, the difference between independent experimental values is about 10 kcal/mol if we neglect the isotope effect. The UBI-QEP value (11 kcal/mol) is between these two.

Klier et al.[16] studied structure sensitivity of methane dissociation on palladium single crystals and reported an apparent activation energy of about 8 kcal/mol for Pd(111), which is about 8.5 kcal/mol lower than the thermal barrier. The activation energy is close to the value predicted by the UBI-QEP method.

Frennet reported that among Cu, Rh, Pd, and Ni films, copper is least reactive.[23] This agrees with a higher value of the activation energy predicted by the UBI-QEP value, which disagrees with the measurements of Alstrup et al.[13] These authors reported an exceedingly high value of 48 kcal/mol. The data on methane chemisorption are summarized in Table 2.

H−H Dissociation. This reaction was not used in the profiling methods discussed in this paper because of the uniqueness of its core fragment (see below), since any conclusion would be too sensitive to a single error. Therefore, we did not analyze the available experimental data as comprehensively as for methane dissociation. Table 3 lists the values for H−H dissociation at the surface and the values of apparent activation energies predicted by the UBI-QEP method. The latter values were calculated by us using the formula[6]

$$E_{H2,g} = (^1/_2)(D_{H-H} - 1.5Q_H - Q_{H2})$$

where $D = 104$ kcal/mol is the H−H bond energy in the gas phase, Q_H is the heat of atomic hydrogen chemisorption, and Q_{H2} is the heat of dihydrogen adsorption. The values of Q_H and Q_{H2} are available from ref 2. Most of the experimental

TABLE 4: Experimental and Calculated Activation Energies (in kcal/mol) for Hydrogen Recombination

	Cu(111)	Ni(111)	Pd(111)	Pt(111)	Rh(111)	Ru(001)	Ir(111)	Fe(110)
experiment	11.5−12[a]	19, 22[b]	20.8[c]	9−23[d]	18.6[e]	24[f]	18[g] 17 ± 2[h]	25[i]
UBI-QEP value	10.6	23.4	22.2	21.1	21.1	27.9	17.6	24.5

[a] The value for Cu(111) should be close to other low-index planes Cu(100) and Cu(110); for these surfaces the experimental values are 11.5 (ref 28a) and 12 (ref 28b), respectively. [b] Reference 29 (two TPD peaks for different states of hydrogen). [c] Reference 30. [d] Reference 31 (data from different sources vary over a broad range). [e] Reference 32. [f] Reference 33. [g] TPD data (ref 34a). [h] Data from molecular beam relaxation spectroscopy and time-resolved specular helium scattering (ref 34b). [i] Reference 27.

values in Table 3 are from the review papers by Shustorovich, Bell, and Sellers,[5,24] and we did not check their comparisons.

Whitten and Yang[21] reviewed various results of theoretical studies (semiempirical and ab initio) of chemisorption reactions and compared them to experimental findings when they were available. Specifically, H_2 chemisorption on Ni(111), which has long been an interest of theory, is discussed in detail. They cited various experimental studies all agreeing that the apparent activation barrier for the reaction $H_{2,g} \rightarrow 2H_s$ is 1−2.3 kcal/mol. The same values were confirmed by semiempirical and ab initio calculations. As can be seen, there is a good agreement with experiment. However, except for Cu(111), all the values of dissociative adsorption are comparable to the accuracy of calculations; hence, a comparison of the rankings does not make sense. The value for Cu(111) is somewhat higher than the corresponding values for other surfaces both in experiments and in calculations.

H_2 Desorption. Like H_2 dissociation, this reaction was not used by our profiling methods for the same reasons. Table 4 summarizes the available published TPD and other data.[28−34] The UBI-QEP values of activation energies for the recombination on the surface and the apparent activation energies for recombination with H_2 desorption are the same. As can be seen, the agreement with experiment is generally good in terms of absolute values and in terms of the comparative reactivity of metal surfaces assuming that the declared error in the calculation is 3 kcal/mol. However, there is some discrepancy, which can be attributed to defects either of the UBI-QEP method or of experiment; according to Zaera,[35] TPD is a "less than ideal technique for kinetic studies because of the nonisothermal nature of experiments which leads to correlated changes in coverages and rates".

H−O Dissociation. For these reactions, Hei et al.[2] proposed corrected values used in calculations. Adsorbed water dissociation into OH_s and H_s on Cu(111) was reported to have an activation energy of 27 kcal/mol.[36,37] The "classical" UBI-QEP value is 25.4, and a value corrected to account for hydrogen bonds (which was used in this paper) is 17.6 kcal/mol. The reaction of H_s with O_s on Cu(111) to give surface hydroxyl was reported to have an activation energy of 22.2 ± 2.5 kcal/mol.[38] The "uncorrected" and "corrected" values are 20.8 and 10.7 kcal/mol, respectively. So the corrections for hydrogen bonds seem to be superfluous, although they sometimes provide better agreement of calculated heats of hydroxyl chemisorption with experiment. Hue et al.[2] claimed that no quantitative change in metal comparative properties should be expected, so we used the corrected values. The same reaction was discussed in a review paper by Shustorovich and Sellers.[6] They mentioned that on Pt(111) the experimental activation energy should be lower than 13 kcal/mol[39] and provided a UBI-QEP value of 10 kcal/mol. Hei et al.[2] report a "corrected" value of 25.3 kcal/mol, which seems overestimated.

H−O Formation. Paredes Olivera et al.[40] have found coincidence of calculated and experimental[41] activation energies for the reaction $CH_3O_s + H_s \rightarrow CH_3OH_s$, which are 12.6 and 13.8 kcal/mol, respectively, for Rh(111).

Fisher et al. have found that the reaction $H_s + OH_s \rightarrow H_2O_s$ on Pt(111) has an activation barrier of 8 kcal/mol,[42] which agrees well with the UBI-QEP value of 11.2 kcal/mol. In this case, the correction for hydrogen bonds worked well. Also, the value reported by Anton and Cadogan[39] is 16 ± 5, which agrees with the calculated value and does not agree with the alternative experimental value.

Recombination of CO and O. The experimental data for CO_s recombination with O_s vary significantly because this reaction is usually studied as a step of CO oxidation and it is difficult to extract reliable information about the activation energy of a single step from multiple-step kinetics. Thus, for this reaction on Pt(111), Gland and Kollin,[43] Campbell et al.,[44] Franz et al.,[45] and Zaera et al.[35] reported the following values of apparent activation energies for the $CO_s + O_s \rightarrow CO_{2,g}$ reaction: 40, 24.1, 23, and 9 kcal/mol, respectively. Considering that ultrahigh vacuum (UHV) molecular beam surface scattering gave a more accurate prediction (24.1 kcal/mol) than temperature-programmed reaction spectroscopy (40 kcal/mol) and excluding the value of Zaera et al.,[35] which may be inaccurate as pointed out in the paper, we may assume that 23−24 kcal/mol is the "true" value. The respective value in our starting data is 4.8 kcal/mol, and this is easy to reconcile with the experiment because 4.8 is the value for the reaction on the surface $CO_s + O_s \rightarrow CO_{2,s}$. The activation energy for this reaction was estimated as follows. Reaction enthalpy is $\Delta H = Q_{CO} + Q_O - (D_{CO2} - D_{CO}) - Q_{CO2} = -6.4$ kcal/mol, where $D_{CO2} - D_{CO}$ is the energy of C−O bond dissociation in the gas phase and Q_{CO}, Q_O, and Q_{CO2} are the respective heats of chemisorption. Then the activation energy of the surface reaction is $E_a = 0.5[\Delta H + (Q_{CO}Q_O)/(Q_{CO} + Q_O)] = 4.8$ kcal/mol. For the reaction with CO_2 desorption, the activation energy calculated using the same values of Q_{CO}, Q_O, and Q_{CO2} is $E_a = (Q_{CO}Q_O)/(Q_{CO} + Q_O) = 23.2$ kcal/mol, which is in excellent agreement with the experiment. Shustorovich reported the agreement of calculations and experiment for Pd(111) and Rh(111) using about the same data for activation energy calculations.[5] So we may conclude that the data that we used for the surface reaction without carbon dioxide desorption are also correct.

Other Reactions. Morikawa et al. carried out DFT calculations and found that the energy barriers for CO_s dissociation on Ni(111) surface is 1.6 times lower than on Pt(111).[46] This is true of UBI-QEP predictions as well.

We found the elementary step $C_2H_{6,s} \rightarrow 2CH_{3,s}$ dubious in view of ethane hydrogenolysis studies.[47−50] Even if we consider this step elementary, the activation energy of zero for Fe(110) sounds strongly underestimated.

The activation barrier for α-hydride elimination from methyl over Pt(111) suggested by H−D exchange in methyl groups is below 10 kcal/mol,[51] whereas the UBI-QEP value is 25.7 kcal/mol. The reverse reaction ($CH_{2,s} + H_s \rightarrow CH_{3,s}$) has an

TABLE 5: Elementary Steps and Their Core Fragments

core fragment	step numbers from Table 1	*N* [a]
M−C−×−H−M	1, 2, 3, 4, 46, 55, 70	7
M−×−C−H−×−M	85, 86, 87, 88, 130, 139, 154	7
M−×−C−H−×−C−M	5, 6, 7, 8, 9, 10, 13, 14, 48, 50, 52, 59, 64, 67, 74, 75, 77, 78, 89, 90, 91, 92, 93, 94, 97, 98, 132, 134, 136, 138, 143, 148, 151, 158, 159, 161, 162	37
M−×−H−O−×−C−M	21, 125, 61, 24	4
M−H−×−O−C−×−M	105, 41, 145, 108	4
M−×−C−C−×−M	11, 12	2
M−C−×−C−M	95, 96	2
M−×−C−O−×−C−M	15, 16, 17, 18, 47, 49, 58, 65, 66, 99, 100, 101, 102, 131, 133, 142, 149, 150	18
M−C−×−O−O−×−M	19, 53	2
M−×−C−O−×−O−M	103, 137	2
M−×−O−C−×−H−M	28, 106, 35, 33	4
M−O−×−C−H−×−M	22, 119, 112, 117	4
M−×−H−O−×−M	20, 80, 82, 144	4
M−H−×−O−M	104, 164, 166, 60	4
M−C−×−O−M	25, 26, 114, 115, 44, 63, 71	7
M−×−C−O−×−M	109, 110, 30, 31, 128, 147, 155	7
M−C−×−H−O−×−M	27, 29, 32, 34, 40, 42, 43, 51, 56, 57, 69, 72, 73	13
M−×−C−H−×−O−M	111, 113, 116, 118, 124, 126, 127, 135, 140, 141, 153, 156, 157	13
M−C−×−H−H−×−M	36, 37, 38, 39, 68, 76	6
M−×−C−H−×−H−M	120, 121, 122, 123, 152, 160	6
M−×−O−H−×−O−M	54, 138, 79, 163	4
M−H−×−H−O−×−M	81, 167	2
M−×−H−H−×−O−M	165, 83	2
M−×−H−H−×−M	84	1
M−H−×−H−M	168	1

[a] *N* Is the overall number of elementary steps.

experimental activation barrier of 6 kcal/mol or less,[51b] and the UBI-QEP value is 6.4 kcal/mol, which agrees well with the experimental value.

Conclusion on the Accuracy of the Calculated Activation Energies. Overall, we find that the theoretical activation energies found by Hei et al.[2] correspond adequately to experiments. Sometimes there are discrepancies. Even when we see disagreement between the calculated values and observations, we decided to leave the initial data untouched. If some entries of Table 1 are wrong, they reflect the errors inherent in the method. Therefore, when these methods lead to strange conjectures, one can identify the source of errors and make appropriate corrections systematically rather than change any specific value. The replacement of wrong values in Table 1 with those that currently seem correct may generate unrecoverable errors because their source would be barely understandable.

Before proceeding to our own findings, we stress that, in general, clustering is somewhat insensitive to isolated errors because clustering relies on intermetal distance, which is the Euclidean distance in a 168-dimensional space. Profiling can be more sensitive to isolated errors when the number of reactions that satisfy a core fragment is small. No matter how reliable are the initial data, the immediate output of any generalization method is always hypothetical and in need of further tests.

Features of Reactions

Clustering can be done with the raw reactions data, but we also seek generalized explanations for the differences among catalysts, which motivate the following definitions of generalized features of elementary steps.

Core Fragments. One type of feature relates to the structure of the transition state. If each surface species is defined in terms of the valence-bond scheme, one can find which bonds are formed and which are broken. For instance, we interpret the step $CH_3 \rightarrow CH_2 + H$ from Table 1 as follows:

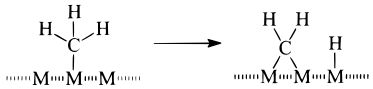

The same step can be depicted by a single image that shows which bonds are formed (thick lines) or broken (a dashed line):

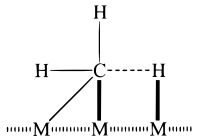

If we remove the bonds that remain unchanged, then we have a simpler image, which may be common to several elementary steps.

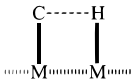

The same image can be depicted with a linear notation that we use throughout the article:

$$M-C-\times-H-M$$

where "−" denotes a bond being formed and "−×−" denotes a bond being broken. We call such an image the *core fragment* of a step. For all the steps in Table 1, we found 25 different core fragments, which are listed in Table 5.

Core fragments express a similarity between the transition states of different steps by highlighting the specific bonds formed or broken during the reaction. Each step has a specific core fragment, but the assignment of a core fragment to a step is somewhat informal because one has to know or hypothesize how the species participating in the step are coordinated to the surface. We assume that the transition state is as simple as

possible; that is, it involves the fewest bonds formed and broken. Another source of uncertainty is that a step may have different transition states. For instance, step 50 in Table 1, $CH_3O + CH_2 \rightarrow CH_3 + CH_2O$, can either break one C−O bond and form another C−O bond or break and form a C−H bond. Another example is step 54 ($CH_3O + OH \rightarrow CH_3OH + O$), which can either be O−H breaking/O−H forming or C−O breaking/C−O forming. By symmetry, their reversed steps 134 and 138 are also ambiguous. (These steps were detected automatically using a component of the computer program MECHEM.[52]) In these cases, we consulted the authors on the activation energies[2] to determine which transition states were used in their calculations. The core fragments of all the steps are shown in Table 1.

To contrast different catalysts, we used only those features that could be assigned to at least four elementary steps because we considered that any smaller number would lead to unreliable conclusions. Therefore, we discarded some of the infrequent core fragments in Table 5.

Species Formation/Consumption. Another type of feature used to contrast various families of transition metal catalysts is the formation of a species or its consumption in a step. We grouped the steps according to the species formed or consumed. Each step may belong to up to four groups, since every step has at most two reactants and at most two products. There are 23 species in the steps from Table 1, so the maximum number of features of the type "a step consumes a species X" or "a step forms a species X" is 46. As in the case of core fragments, we keep only those features that match at least four reactions: formation or consumption of CH_3OH, H_2O, H_2, OH, HCOO, O, HCO, CH_2O, CO, CH_3O, CO_2, C, CH, CH_2, H, CH_3, or CH_4 (overall, 34 features).

Bond Formation/Breaking. Other plausibly useful features refer to single bonds that are formed or broken. However, our computational experiments with these features gave results that are uninformative or misleading probably because all bonds formed and broken contribute to the activation energy barrier, which obscures the effect of any single bond change. This is why we introduced the core-fragment features instead. Bond-breaking/formation features might be very informative if, instead of the activation energies of elementary steps, one had the values of bond energies for species adsorbed on different metal catalysts.

Results and Discussion

Our study involved these steps.

(1) Find clusters that express the broad similarities (or differences) among the metals by using hierarchical clustering algorithms.

(2) Find the feature that best contrasts the two clusters of metals formed at each branch point in the hierarchy.

(3) Find the features that best contrast each metal from the remaining metals.

(4) Find the feature that best contrasts each pair of metals.

Clustering. How do the eight metals compare in terms of the activation energies of the elementary steps? Classical hierarchical clustering can answer this question. Each metal determines a point in a 168-dimensional space in which each dimension corresponds to a different step's activation energy. We define the similarity between two metals as the reciprocal of the Euclidean distance between them; the latter values are shown in Figure 1. The pairs of metals that are less similar are on the top-right corner, and those that tend to be more similar are closer to the diagonal. We shaded the figure to show three degrees of similarity: (a) a distance shorter than 100 (similarity, white region); (b) a distance between 100 and 200 (medium similarity, light shading); (c) a distance longer than 200 (dissimilarity, dark shading). The pairs of most similar metals are (Pd and Pt), (Pd and Ir), and (Rh and Ru). The pairs of most dissimilar metals are (Fe and Pt) and (Cu and Fe). Medium distances are not too informative because of the possible errors in the starting data and some arbitrariness in the choice of a distance measure. We used both the single-link and complete-link clustering methods, whose results appear in Figure 2.

	Ni	Ru	Rh	Pd	Ir	Pt	Cu	
	90.20	99.30	116.1	184.1	167.1	208.3	225.2	Fe
		65.60	57.40	127.3	106.9	147.8	152.8	Ni
			47.70	101.2	92.50	128.6	169.5	Ru
				78.40	57.70	103.0	138.9	Rh
					35.30	35.60	132.1	Pd
						55.80	121.7	Ir
							119.6	Pt

Figure 1. Euclidean distance between metals.

Both complete-link and single-link clustering uncover hierarchical families of metal catalysts (clusters) that express similar behavior. The complete-link clustering suggests that Cu, Pt, Ir, and Pd are similar. Indeed, methanol synthesis from syngas coupled with the water gas shift reaction is known to occur more rapidly over Cu catalysts.[53] Lee and Ponec suggested dividing the group VIII transition elements and copper into two categories: those to the left and right of the diagonal across three periods of group VIII:[54]

	VIII			IB
	Fe		Ni	Cu
	Ru	Rh	Pd	
		Ir	Pt	

The elements to the right (Cu, Pt, Ir, and Pd) seem to be the best catalysts for methanol synthesis, unlike those to the left and on the diagonal (Fe, Ni, Rh, and Ru). These two groups correspond to the first major branching in the complete-link output. Cu, Pt, Ir, and Pd do not dissociate CO or do so too slowly. Conversely, Fe, Ni, Rh, and Ru are favorable for CO dissociation and synthesis of higher hydrocarbons in the Fischer−Tropsch reaction. Of course, the similarity of metals belonging to the same cluster is conditional. Other distance measures or enlargement of the starting data set might result in a different hierarchy of metals. However, the usefulness of the method is in finding new, plausible, and interesting hypotheses that gain further strength if supported in part by the available experimental data.

The single-link hierarchy quickly separates Cu and Fe from Rh, Ru, Ni, Pt, Ir, and Pd, which are known as good hydrogenation catalysts. The activity of Cu in this reaction is at least an order of magnitude lower than the activities of group VIII metals, and the activity of Fe is at best half that of the other metals.[55]

In the water gas shift reaction, the relative activities of supported metal catalysts in terms of turnover numbers at 300 °C and standard conditions[56] are in the following order.

Cu	≫	Ru	>	Ni	>	Pt	>	Fe	>	Pd	>	Rh	>	Ir
3800		60		32		20		5		4		3		1

This confirms that Cu can be very different from the other metals

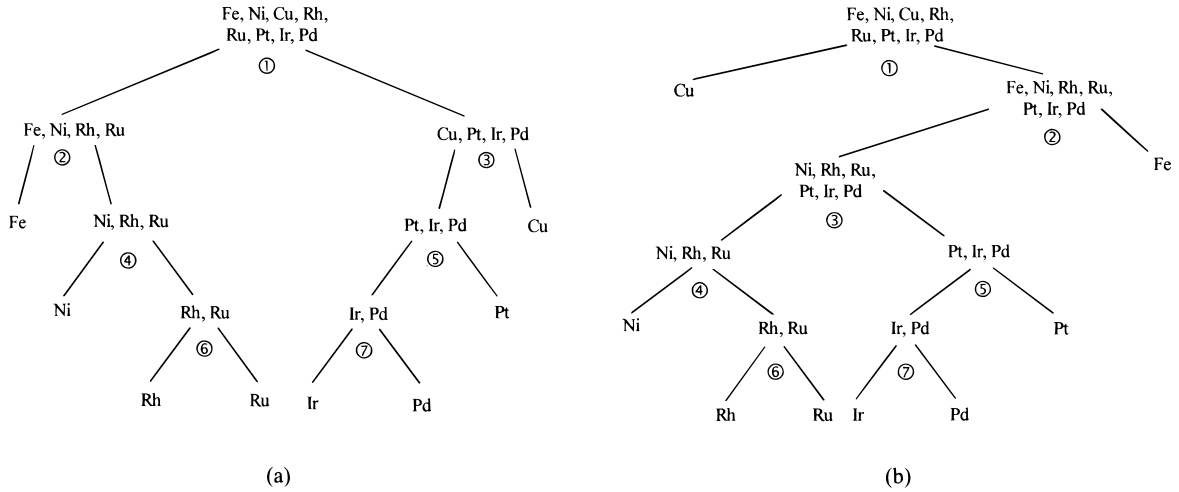

Figure 2. Hierarchical clustering of metals: (a) complete-link clustering; (b) single-link clustering.

TABLE 6: Annotation of the Trees Obtained by Single-Link and Complete-Link Clustering[a]

n	clusters to contrast	single best contrasting feature (core fragment)	overlap	range of activation energy	E_{mean}	E_{med}	σ	*N*
1[b]	Cu is better than Fe, Rh, Ru, Ni, Pt, Ir, Pd	M−×−C−O−×−M	0.25	0−45.40	7.46	0	15.58	7
				0−50.50	19.36	15.20	13.66	49
1[c]	Fe, Ni, Rh, Ru is worse than Cu, Pt, Ir, Pd	M−×−C−O−×−M	0.36	8.00−49.60	24.10	21.75	10.83	28
				0.00−50.50	11.65	6.75	14.95	28
2[b]	Fe is worse than Rh, Ru, Ni, Pt, Ir, Pd	M−×−O−C−×−H−M	0.05	20.4−28.80	23.50	22.40	3.41	4
				0−20.90	8.00	5.95	7.59	24
2[c]	Fe is worse than Ni, Rh, Ru	M−×−O−C−×−H−M	0.09	20.40−28.80	23.50	22.40	3.41	4
				1.00−20.90	11.49	11.25	6.75	12
3[b]	Pt, Ir, Pd is better than Rh, Ru, Ni	M−×−O−C−×−H−M	0.34	0−17.90	4.51	0	6.72	12
				1−20.90	11.49	11.25	6.75	12
3[b]	Pt, Ir, Pd is better than Rh, Ru, Ni	M−×−H−O−×−M	0.34	6.2−21.50	11.94	11.40	4.60	12
				2.8−20.70	15.18	16.30	5.02	12
3[c]	Cu is better than Pt, Ir, Pd	M−×−C−H−×−M	0.29	0.00−30.80	9.04	3.70	11.89	7
				5.60−39.70	17.55	13.20	12.08	21
6[d]	Ru is worse than Rh	M−×−H−O−×−M	0.25	15.5−19.90	17.25	16.80	1.77	4
				8.2−16.80	12.93	13.35	3.12	4

[a] *n* is the number of a binary split in Figure 2. E_{mean}, E_{med}, and σ are the mean, median, and standard deviation of the activation energies, all in kcal/mol. *N* is the number of elementary steps used. [b] Single-link. [c] Complete-link. [d] Both methods.

in the series, which is consistent with its early divergence in the tree obtained by single-link clustering.

Annotating the Tree for Best Contrasting Features. Clustering reveals which metals are similar or different, but says nothing about how or why. The core fragments and other features introduced above enable addition of explanatory annotations to a hierarchical clustering at its branch points. The annotations use the CAPP method, which compares each cluster individually with every other cluster in the comparison set and then minimizes the number of features needed to profile the clusters. The comparison set is formulated by the user and can be as small as two clusters, in which case the profiles consist of a single feature that best contrasts the pair of clusters.

We found the resulting profiles harder to interpret when they mixed different types of features, so our final runs with CAPP considered only one feature type at a time (usually just the core fragments).

Table 6 lists the annotations of the complete-link and single-link clustering using only the core-fragment features and considering that each branch in the hierarchy corresponded to its own two-cluster comparison set. The listed overlaps (ranging from 0 to 1) characterize the strengths of the contrasts; the smaller the overlap, the better is the contrast. Some branches in the hierarchies are not annotated because the difference between the two clusters is weak, because of either a high overlap of activation energy values or a small difference between the mean activation energies.

CAPP was also used to globally minimize the use of features across all branches in a hierarchy. This procedure led to using only the two core-fragment features M−×−O−C−×−H−M and M−H−×−O−C−×−M, which contrast all the sibling clusters (clusters at a branching point) within a 0.5 overlap. This implies that any overall reaction that occurs via steps with these core fragments (especially if these steps are slow) may be sensitive to the choice of transition metal catalyst.

Our experiments with the features relating to the formation or consumption of specific species showed that, either with or without global minimization, the feature "elementary step forms CH_3OH" is the best discriminator of the clusters. In the case of global minimization, the tree can be annotated with this feature alone, although the maximum overlap is too high (0.67). Figure 3 shows the complete-link clustering annotated with the mean values of the activation energies for elementary reactions that form methanol. All other features are less informative. That is, different types of activation or formation reactions respond differently to the choice of a metal.

Initially, it was somewhat surprising that Cu has the second highest (among all metals, but after Fe) mean activation energy barrier over all elementary steps producing methanol because it is known to be the most active in the methanol synthesis process. On the other hand, not all of the elementary steps that

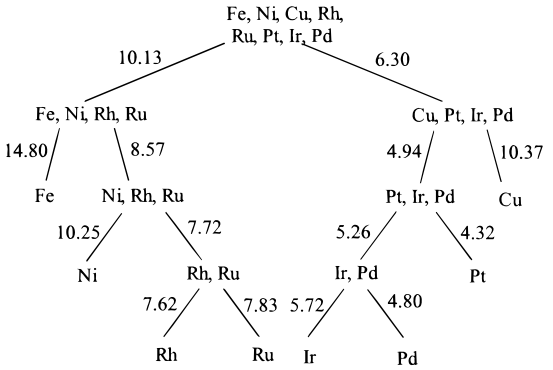

Figure 3. Complete-link tree annotated with the mean values of the activation energies for the elementary reactions of methanol formation.

produce methanol are important for the methanol synthesis process. These methanol-forming steps differ largely in the source of hydrogen to be added to CH_3O and in the transition states (and hence, core fragments):

$$CH_3O + CH_3 \rightarrow CH_2 + CH_3OH$$

$$CH_3O + OH \rightarrow CH_3OH + O$$

$$CH_2O + CH_3O \rightarrow CH_3OH + HCO$$

$$HCO + CH_3O \rightarrow CH_3OH + CO$$

$$CH_3O + H \rightarrow CH_3OH$$

$$CH_3 + H_2O \rightarrow CH_3OH + H$$

Thus, the first reaction in this list is unfavorable over Cu surface (27.1 kcal/mol). Another possible explanation is that the final stage of methanol synthesis might not control its rate.

As can be seen from Table 6, the sharpest contrast (0.05 overlap) is between Fe and other group VIII transition metals because of the substantial difference in the behavior of Fe in reactions with the M−×−O−C−×−H−M core fragment. On Fe, the activation energies of elementary steps involving that core fragment range from 20.4 to 28.8 kcal/mol, whereas for the other group VIII transition metals, they range from 0 to 20.9 kcal/mol. The next-sharpest contrast is between Fe and the set Ni, Rh, and Ru, which is interesting because complete-link clustering places these four metals in the same cluster at the first branch, implying that these four metals are broadly similar but not in steps with the M−×−O−C−×−H−M core fragment.

Other sharp contrasts involve Cu. The core fragment M−×−C−O−×−M distinguishes Cu from all group VIII metals including Fe. The core fragment M−×−C−H−×−M distinguishes Cu from its peers in the (Cu, Pt, Ir, Pd) cluster. Ru and Rh, which are very similar and form a (Ru, Rh) cluster in all the methods we tried, nevertheless differ substantially on the M−×−H−O−×−M core fragment, although there are only four such reactions in our data set. This means that if some reaction occurs via a slow step with this core fragment, then the choice between Rh and Ru catalysts may be significant.

Each of the two core fragments M−×−H−H−×−M and M−H−×−H−M corresponds to only one possible reaction. In this case, the contrasts among metals are seen without any special program, and therefore, we excluded these two core-fragment features from the start. On these two reactions, Cu behaves quite differently from the other metals. Cu has the lowest activation energy in the M−×−H−H−×− process (10 versus 17−24 kcal/mol for the other metals) and the highest activation energy in the M−H−×−H−M process (15 versus 5.6−11 kcal/mol for the others). The metals can be arranged in an activity series for H−H bond breaking,

Cu	>	Ir	>	Pt, Rh	>	Ni	∼	Pd	>	Fe	>	Ru
15.4		11.4		9.5		8.2		8.8		7.0		5.6

and for H−H bond formation,

Cu	<	Ir	<	Pt, Rh	<	Pd	∼	Ni	<	Fe	<	Ru
10.6		17.6		21.1		22.2		23.4		24.5		27.9

The activity series for H−H dissociation changes slightly if we consider direct dissociative chemisorption from the gas phase (see Table 2).

Finding Features that Contrast Each Catalyst from All Others. Hierarchical clustering methods accept a list of metals and create a taxonomic tree that expresses broad similarities among the metals. Sometimes this leads to peculiarities if the metals are not uniformly similar. For example, Figure 3 shows that Cu is closer in the CH_3OH formation property to the (Fe, Ni, Rh, Ru) cluster than to Pt, Ir, and Pd. Alternatively, we can regard the metals as a typology (i.e., as an unstructured list of peers) and ask how each metal differs from all the other metals, without grouping them. We applied the CAPP program to profile each of the eight metals while allowing only core-fragment features. Table 7 lists these profiles.

Sometimes one feature is enough to contrast one metal from the rest, as in the case of Cu, Pd, Pt, and Ir in Table 7. The Cu profile is the sharpest; steps with the core fragment M−×−C−H−×−M are much faster over Cu than over each of the other metals (0.29 overlap). Other contrasts are less sharp but still can be useful to express the unique (in this context) capabilities (or disabilities) of metals.

Finding Features that Contrast Pairs of Catalysts. Another interesting question is "What feature best contrasts a given pair of metals?" This question calls neither for clustering of the metals nor for consideration of the influence of other metals not in the pair. Interestingly, if we include only the core fragments that correspond to at least five steps in our data set and reject any contrasts that are not sharp, then only three core fragments are used: M−×−C−O−×−M, M−×−C−H−×−M, and M−C−×−H−H−×−M. Among these three, M−C−×−H−H−×−M is used only once to distinguish between Ni and Rh, and the overlap is high (0.67). The M−×−C−H−×−M core fragment is used several times, but the M−×−C−O−×−M core fragment appears the most and has lower overlaps. This suggests that if a reaction mechanism involves a step with this core fragment, then a difference in metal behavior should be more apparent. Table 8 lists these results.

Sometimes we see "ideal" contrasts that have an overlap of zero. Unfortunately, these are unreliable from a statistical standpoint. For example, if we allow the core-fragment features that match only four steps, then we see the following ideal contrasts for metal pairs:

(1) Cu is better than Ru for M−×−H−O−×−M.

(2) Ru is worse than Ir for M−×−H−O−×−M.

(3) Cu is better than Fe for M−H−×−O−C−×−M.

(4) Pd is better than Fe for M−H−×−O−C−×−M and M−×−O−C−×−H−M.

(5) Pt is better than Fe for M−H−×−O−C−×−M and M−×−O−C−×−H−M.

(6) Rh is better than Fe for M−×−O−C−×−H−M.

(7) Ru is better than Fe for M−×−O−C−×−H−M.

TABLE 7: Contrasting Metals by Core-Fragment Features[a]

metal	best contrasting features (core fragments)	overlap	range of activation energy	E_{mean}	E_{med}	σ	N
Cu	M−×−C−H−×−M (better than for all others)	0.29	0.00−30.80	9.04	3.70	11.89	7
Ni	M−×−C−O−×−M (worse than for Cu, Pt, Pd, and Ir and better than for Fe)	0.67	8.00−35.40	21.17	20.90	10.30	7
	M−C−×−H−H−×−M (worse than for Pd, Pt, Rh, and Ir and better than for Cu and Ru)		9.50−27.20	17.95	18.20	6.81	6
Pd	M−×−C−O−×−M (worse than for Cu and Pt and better than for Fe, Ni, Rh, Ru, and Ir)	0.58	3.10−46.10	13.54	7.30	13.73	7
Pt	M−×−C−O−×−M (worse than for Cu and better than for Cu, Ni, Rh, Ru, Pd, Ir, and Fe)	0.58	0.00−50.50	10.59	4.80	16.72	7
Rh	M−×−C−O−×−M (worse than for Cu, Pt, Pd, and Ir and better than for Fe and Ru)	0.67	8.70−40.00	20.14	18.60	9.21	7
	M−C−×−H−H−×−M (better than for Cu, Ni, Pd, Pt, and Ru)		6.50−25.80	15.25	15.75	6.57	6
Ru	M−×−C−H−×−M (worse than for Cu, Ni, Pd, Pt, Rh, and Ir)	0.58	9.90−45.40	23.01	21.70	10.31	7
	M−×−C−O−×−M (worse than for Cu, Pt Pd, Rh, and Ir and better than for Fe)		9.70−39.40	22.43	21.80	9.35	7
Ir	M−×−C−O−×−M (worse than for Cu, Pd, and Pt and better than for Fe, Ni, Rh, and Ru)	0.58	3.80−44.00	15.00	10.40	12.25	7
Fe	M−×−C−H−×−M (worse than for Cu, Ni, Pd, Pt, Rh, and Ir)	0.43	5.30−44.70	22.97	21.90	10.92	7
	M−×−C−O−×−M (worse than for Cu, Pd, Pt, Rh, Ru, and Ir)		20.60−49.60	32.67	32.00	9.49	7

[a] E_{mean}, E_{med}, and σ are the mean, median, and standard deviation of the activation energies, all in kcal/mol. N is the number of elementary steps used. Every feature must correspond to at least five reactions.

TABLE 8: Contrasts of Metals Pairs by Core-Fragment Features with an Overlap Smaller than 0.3[a]

metal	best single contrasting core fragment	overlap	range of activation energy	E_{mean}	E_{med}	σ	N
Cu	M−×−C−O−×−M	0.15	0.00−45.40	7.46	0.00	15.58	7
Ni			8.00−35.40	21.17	20.90	10.30	7
Cu			0.00−45.40	7.46	0.00	15.58	7
Rh			8.70−40.00	20.14	18.60	9.21	7
Cu			0.00−45.40	7.46	0.00	15.58	7
Ru			9.70−39.40	22.43	21.80	9.35	7
Cu			0.00−45.40	7.46	0.00	15.58	7
Fe			20.60−49.60	32.67	32.00	9.49	7
Ir			3.80−44.00	15.00	10.40	12.25	7
Fe			20.60−49.60	32.67	32.00	9.49	7
Pd			3.10−46.10	13.54	7.30	13.73	7
Fe			20.60−49.60	32.67	32.00	9.49	7
Pt			0.00−50.50	10.59	4.80	16.72	7
Ru			9.70−39.40	22.43	21.80	9.35	7
Pt			0.00−50.50	10.59	4.80	16.72	7
Fe			20.60−49.60	32.67	32.00	9.49	7
Cu	M−×−C−H−×−M	0.29	0.00−30.80	9.04	3.70	11.89	7
Pd			9.00−39.70	19.16	15.40	11.76	7
Cu			0.00−30.80	9.04	3.70	11.89	7
Pd			5.60−38.00	17.41	13.20	12.73	7
Cu			0.00−30.80	9.04	3.70	11.89	7
Ir			6.40−36.70	16.09	12.60	11.52	7
Cu	M−×−C−O−×−M		0.00−45.40	7.46	0.00	15.58	7
Pd			3.10−46.10	13.54	7.30	13.73	7
Cu			0.00−45.40	7.46	0.00	15.58	7
Ir			3.80−44.00	15.00	10.40	12.25	7
Ni			8.00−35.40	21.17	20.90	10.30	7
Pt			0.00−50.50	10.59	4.80	16.72	7
Pt			0.00−50.50	10.59	4.80	16.72	7
Rh			8.70−40.00	20.14	18.60	9.21	7
Rh			8.70−40.00	20.14	18.60	9.21	7
Fe			20.60−49.60	32.67	32.00	9.49	7

[a] E_{mean}, E_{med}, and σ are the mean, median, and standard deviation of the activation energies, all in kcal/mol. N is the number of elementary steps used. Every feature must match at least five reactions.

(8) Ir is better than Fe for M−H−×−O−C−×−M and M−×−O−C−×−H−M.

In this context, *better* and *worse* mean that the metal has lower and higher activation energies of steps, respectively.

As we see, the core fragments M−H−×−O−C−×−M, M−×−O−C−×−H−M, and M−×−H−O−×−M are the best discriminators among the infrequent core fragments, and Fe shows the most extreme properties, although it belongs to group VIII (unlike Cu).

If we increase the lower limit for the steps attributable to a core fragment to 5, then the contrasts become less pronounced but statistically more reliable. In this case, the best discriminators

are the core fragments M−×−C−O−×−M and M−×−C−H−×−M, and Cu and Fe still stand out as extreme.

This knowledge of contrasts can be useful. For example, in ethane hydrogenolysis, C−C bond scission is known to be a rate-limiting step.[47,48,57,58] However, it remains unclear what specific step among all possible C−C bond scissions is the most important in ethane hydrogenolysis. In other words, the degree of ethane dehydrogenation and the structure of dehydrogenated surface species are still uncertain. Also, the degree of ethane dehydrogenation before C−C bond scission may differ from one metal to another. However, one could predict the relative activities of metals on the basis of knowledge of catalyst behavior in steps with the M−C−×−C−M core fragment. Unfortunately, this is outside the scope of our current data, which contain only two elementary reactions for this core fragment, and this small number does not allow a sound generalization.

Conclusion

The compilation of sets of elementary reactions and their energetics parameters over different metal catalysts, whether determined experimentally or by computational chemistry, affords an unexplored chance to uncover more general qualitative relations among metals. Some basic questions of interest are which metals are different, which are similar, and how they are different or similar. Answers to these questions can guide the selection of promising catalysts for a given reaction, prior to carrying out kinetics or other experiments.

This article has applied classical hierarchical clustering and recently developed profiling methods to published data on 168 elementary steps relevant to methane re-forming and their activation energies. The core fragments of the transition states of each of the steps were identified, together with other features that proved less useful. One result consists of hierarchical clusterings of the metals, annotated at branch points with the core fragment that best contrasts the diverging clusters. Second, we obtained a concise profile for each metal by contrasting it with the other seven metals. Finally, we listed the single best contrasting feature for many pairs of metals. These results are largely consistent with previous experimental observations, which gives confidence in the methods' suitability for prediction.

References and Notes

(1) *Knowledge discovery* is a subfield of artificial intelligence that deals with the design of computer programs to assist their users in finding novel, interesting, plausible, and intelligible knowledge about the object of study. See, for example, the following. Valdés-Pérez, R. E. *Artif. Intell.* **1999**, *107*, 335.

(2) Hei, M. J.; Chen, H. B.; Yi, J.; Lin, Y. J.; Lin, Y. Z.; Wei, G.; Liao, D. W. *Surf. Sci.* **1998**, *417*, 82.

(3) Hartigan, J. A. *Clustering Algorithms*; Wiley: New York, 1975.

(4) Valdés-Pérez, R. E.; Pericliev, V. *Int. J. Human Comput. Stud.*, submitted.

(5) Shustorovich, E.; Sellers, H. *Surf. Sci. Rep*. **1998**, *31*, 1.

(6) Shustorovich, E. *Adv. Catal.* **1990**, *37*, 101.

(7) Bell, A. T. *Metal-Surface Reaction Energetics: Theory and Applications to Heterogeneous Catalysis, Chemisorption and Surface Diffusion*; VCH: Weinheim, 1991; pp 191−227.

(8) Verheij, L. K.; Hugenschmidt, M. B. *Surf. Sci.* **1998**, *416*, 37.

(9) Goodman, D. W. *J. Chem. Phys.* **1996**, *100*, 13090.

(10) Somorjai, G. A. *Introduction to Surface Chemistry and Catalysis*; Wiley: New York, 1994.

(11) Johnson, D. F.; Weinberg, W. H. *Science* **1993**, *261*, 76.

(12) Campbell, C. T.; Sun, Y. K.; Weinberg, W. H. *Chem. Phys. Lett.* **1991**, *179*, 53.

(13) Astrup, I.; Chorkendorf, I.; Ullmann, S. *Surf. Sci.* **1992**, *264*, 95.

(14) (a) Beebe, T. P., Jr.; Goodman, D. W.; Kay, B. D.; Yates, J. T. *J. Chem. Phys.* **1987**, *87*, 2305. (b) Lee, M. B.; Yang, Q. Y.; Tang, S. L.; Ceyer, S. T. *J. Chem. Phys.* **1986**, *85*, 1693. (c) Lee, M. B.; Yang, Q. Y.; Ceyer, S. T. *J. Chem. Phys.* **1987**, *87*, 2724−2741. (d) Beckerle, J. D.; Johnson, A. D.; Yang, Q. Y.; Ceyer, S. T. *J. Chem. Phys*. **1989**, *91*, 5756.

(15) Schoofs, G. R.; Arumainayagam, C. R.; McMaster, M. C.; Madix, R. J. *Surf. Sci.* **1989**, *215*, 1.

(16) Klier, K.; Hess, J. S.; Herman, R. G. *J. Chem. Phys.* **1997**, *107*, 4033.

(17) Valden, M.; Pere, J.; Hirsimäki, M.; Suhonen, S.; Pessa, M. *Surf. Sci.* **1997**, *377*−*379*, 605.

(18) Seets, D. C.; Reeves, C. T.; Ferguson, B. A.; Wheeler, M. C.; Mullins, C. B. *J. Chem. Phys.* **1997**, *107*, 10229.

(19) Jachimowski, T. A.; Hagedorn, C. J.; Weinberg, W. H. *Surf. Sci*. **1997**, *393*, 126−134.

(20) Zaera, F. *Chem. Rev*. **1995**, *95*, 2651.

(21) Whitten, J. L.; Yang, H. *Surf. Sci. Rep.* **1996**, *218*, 55.

(22) Ukraintsev, V. A.; Harrison, I. *J. Chem. Phys.* **1994**, *101*, 1564.

(23) Frennet, A. *Catal. Rev. Sci. Eng.* **1974**, *10*, 37.

(24) Shustorovich, E.; Bell, A. T. *Surf. Sci. Rep*. **1991**, *253*, 386.

(25) Lloyd, P. B.; Swaminathan, M.; Kress, J. W.; Tatarchuk, B. J. *Appl. Surf. Sci.* **1997**, *119*, 267.

(26) (a) Gale, R. J.; Salmeron, M.; Somorjai, G. A. *Phys. Rev. Lett.* **1977**, *38*, 1027. (b) Salmeron, M.; Gale, R. J.; Somorjai, G. A. *J. Chem. Phys.* **1977**, *67*, 5324. (c) Salmeron, M.; Gale, R. J.; Somorjai, G. A. *J. Chem. Phys.* **1979**, *70*, 2870. (d) Robota, H. J.; Vielhaber, W.; Lin, M. C.; Segner, J.; Ertl, G. *Surf. Sci.* **1985**, *155*, 101.

(27) Kurz, E. A.; Hudson, J. B. *Surf. Sci*. **1988**, *195*, 15.

(28) (a) Rasmussen, P. B.; Holmblad, P. M.; Christoffersen, H.; Taylor, P. A.; Chorkendorff, I. *Surf. Sci.* **1993**, *287*/*288*, 79. (b) Wachs, I. E.; Madix, R. J. *J. Catal.* **1978**, *53*, 208.

(29) Christmann, K.; Behm, R. J.; Ertl, G.; Van Hove, M. A.; Weinberg, W. H. *J. Chem. Phys.* **1979**, *70*, 4168.

(30) Conrad, H.; Ertl, G.; Latta, E. E. *Surf. Sci.* **1974**, *41*, 435.

(31) (a) Christmann, K.; Ertl, G.; Pignet, T. *Surf. Sci.* **1975**, *54*, 365. (b) Salmeron, M.; Gale, R. J.; Somorjai, G. A. *J. Chem. Phys.* **1978**, *70*, 2807. (c) Gdowski, G. E.; Fair, J. A.; Madix, R. J. *Surf. Sci.* **1983**, *127*, 541. (d) Zaera, F. *J. Phys. Chem.* **1990**, *94*, 8350. (e) Lee, W. T.; Ford, L.; Blowers, P.; Nigg, H. L.; Masel, R. I. *Surf. Sci.* **1998**, *416*, 141.

(32) Yates, J. T, Jr.; Thiel, P. A.; Weinberg, W. H. *Surf. Sci.* **1979**, *84*, 427.

(33) Feulner, P.; Menzel, D. *Surf. Sci.* **1985**, *154*, 465.

(34) (a) Engstrom, J. R.; Tsai, W.; Weinberg, W. H. *Surf. Sci.* **1987**, *87*, 3104. (b) Colonell, J. I.; Curtiss, T. J.; Sibener, S. J. *Surf. Sci.* **1996**, *366*, 19.

(35) Zaera, F.; Liu, J.; Xu, M. *J. Chem. Phys.* **1997**, *106*, 4240.

(36) Campbell, C. T.; Daube, K. A. *J. Catal.* **1987**, *104*, 109.

(37) Ovensen, C. V.; Stoltze, P.; Nørskov, J. K.; Campbell, C. T. *J. Catal.* **1992**, *134*, 445.

(38) Mesters, C. M. A. M.; Vink, T. J.; Gijzeman, O. L. J.; Geus, J. W. *Surf. Sci.* **1983**, *135*, 428.

(39) Anton, A. B.; Cadogan, D. C. *Surf. Sci.* **1990**, *239*, L548.

(40) Paredes Olivera, P.; Patritio, E. M.; Selleres, H. *Surf. Sci.* **1995**, *327*, 330.

(41) Solymosi, F.; Berkó, A.; Tarnóczi, T. I. *Surf. Sci.* **1984**, *141*, 533.

(42) Fisher, G. B.; Gland, J. L.; Schmieg, S. J. *J. Vac. Sci. Technol.* **1982**, *20*, 518.

(43) Gland, J. L.; Kollin, E. B. *J. Chem. Phys*. **1983**, *78*, 963.

(44) Campbell, C. T.; Ertl, G.; Kuipers, H.; Segner, J. *J. Chem. Phys*. **1980**, *73*, 5862.

(45) Franz, A. J.; Ranney, J. T.; Jackson, W. B.; Gland, J. L. *J. Phys. Chem. B* **1999**, *103*, 4457.

(46) Morikawa, Y.; Mortensen, J. J.; Hammer, B.; Nørskov, J. K. *Surf. Sci*. **1997**, *386*, 67.

(47) Sinfelt, J. H. *Adv. Catal.* **1973**, *23*, 91.

(48) Sinfelt, J. H. *Catalysis Reviews*; Marcel Dekker: New York, 1970; Vol. 3, pp 175−205.

(49) Zaera, F.; Somorjai, G. A. *J. Phys. Chem.* **1985**, *89*, 3211.

(50) Chen, B.; Goodwin, J. G., Jr. *J. Catal.* **1995**, *154*, 1.

(51) (a) Zaera, F. *Surf. Sci*. **1992**, *262*, 335. (b) Zaera, F. *Catal. Lett*. **1991**, *11*, 95.

(52) (a) Valdés-Pérez, R. E. *J. Comput. Chem.* **1993**, *14*, 1454. (b) Zeigarnik, A. V.; Valdés-Pérez, R. E.; Temkin, O. N. *Langmuir* **1998**, *14*, 4510.

(53) Herman, R. G.; Klier, K.; Simons, G. W.; Finn, B. P.; Bulks, J. P.; Kobylinski, T. P. *J. Catal.* **1979**, *56*, 407.

(54) Lee, G. V. D.; Ponec, V. *Catal. Rev. Sci. Eng*. **1987**, *29*, 183.

(55) Campbell, I. A. *Catalysis at Surfaces*; Chapman and Hall: London, 1988.

(56) Grenoble, D. C.; Estadt, M. M.; Ollis, D. F. *J. Catal.* **1981**, *67*, 90.

(57) Goddard, S. A.; Amiridis, M. D.; Rekoske, J. E.; Cardona-Martinez, N.; Dumesic, J. A. *J. Catal*. **1989**, *117*, 155.

(58) Wang, P.-K.; Slichter, C. P.; Sinfelt, J. H. *J. Phys. Chem.* **1990**, *94*, 1154.